Do laser interferometers absorb energy from gravitational waves?

Yiqiu Ma[1], David G Blair[1], Chunnong Zhao[1] and William Kells[2]

1: School of Physics, University of Western Australia
2: California Institute of Technology

Abstract. In this paper we discuss the energy interaction between gravitational waves and laser interferometer gravitational wave detectors. We show that the widely held view that the laser interferometer gravitational wave detector absorbs no energy from gravitational waves is only valid under the approximation of a frequency-independent optomechanical coupling strength and a pump laser without detuning with respect to the resonance of the interferometer. For a strongly detuned interferometer, the optical-damping dynamics dissipates gravitational wave energy through the interaction between the test masses and the optical field. For a non-detuned interferometer, the frequency-dependence of the optomechanical coupling strength causes a tiny energy dissipation, which is proved to be equivalent to the Doppler friction raised by Braginsky et.al.

E-mail: myqphy@gmail.com, dgblair@gmail.com

1. Introduction

In the gravitational wave research community acoustic gravitational wave detectors have traditionally been understood quite differently from electromagnetically coupled detectors. Following Weber [1], the sensitivity of acoustic detectors was estimated by considering the gravitational wave energy absorbed by the detector. However for laser interferometer gravitational wave detectors a more convenient method of estimation has normally been based on considering the test masses as free masses that experience the gravitational wave spatial strain h of a passing wave. A widely held viewpoint is if the masses are truly free, no energy is extracted from the wave. This free-mass approximation then leads to the idea that electromagnetically coupled gravitational wave detectors do not absorb energy from the passing wave.

The above point of view recalls the debate about the existence of gravitational waves that occurred from 1916 to 1957 [2]. The proof of the reality of gravitational waves was eventually clarified by the sticky-beads thought experiment, which was publicised by Herman Bondi [3]. The argument was presented by Richard Feynman under the pseudonym Mr Smith at a conference in Chapel Hill, North Carolina in 1957. In this thought experiment the viscous interaction of sticky beads on a rod gives rise to heat (as a gravitational wave passes), proving that gravitational waves are able to deposit energy and therefore cannot be a mathematical artifact. This leads to the viewpoint that every practical detector must be a transducer for gravitational waves, converting wave energy into electromagnetic energy, and amplifying it to enable it to be resolved against the inevitable background of instrument noise.

In this paper we discuss the fundamental question of energy absorption in relation to laser interferometer gravitational wave detectors by studying the energy transfer in the interferometers in detail. Our discussion is designed to illuminate fundamental principles. By analyzing the quantum optomechanical interaction process in the interferometer, we try to give a more complete picture about energy absorption process in laser interferometer gravitational wave detectors, which may motivate further innovation in the field.

The standard analysis of laser interferometer gravitational wave detectors begins with the free mass approximation, and there is no doubt that this approximation is very accurate for calculating gravitational wave signals in the electromagnetically coupled detectors constructed to date. In reality, there is a tiny Doppler friction effect which was first discussed by Braginsky et.al [4] in 1967,later applied on the laser interferometer gravitational wave detector by Saulson [5] in 1997 (see the Appendix). Moreover, we will show here that, for a more general detector configuration, the energy absorbed from the gravitational waves depends strongly on the detector configuration.

The first discussion about how an interferometer extracts energy from gravitational waves through the Doppler friction effect was given by Saulson in [5]. This author pointed out that the Doppler interaction with the electromagnetic coupling field, due to gravitational wave strain acting between test masses gives rise to a small viscous

dissipative term due to the strain-induced test mass velocity. It was suggested that any test mass will absorb energy from a gravitational wave via this mechanism. However for a typical wave and a terrestrial detector, it was shown that the Doppler power absorption was infinitesimal $\sim 10^{-40}W$. The reason of the smallness of this effect is because it is a very tiny second order relativistic effect ($\sim (v/c)^2$, in which v is the speed of test mass motion and c is the speed of light). This argument gives us a picture that the mirrors behaves like beads on the sticky rods under the optomechanical interaction.

Besides the Doppler friction effect, for more general interferometer configurations, there is a non-zero optical damping effect which can absorb gravitational wave energy more strongly. This effect allows us to design interferometric gravitational wave detectors which can absorb more energy through the creation of strongly unbalanced sidebands. The energy absorption cross section can also be increased by maximising this optical damping effect. One such scheme is the angular motion gravitational wave detector proposed in [6].

Our analysis shows that the "Doppler friction" energy can also be interpretated as a result of unbalanced Stokes and anti-Stokes sidebands.

In this paper, we first give a analysis on the basic optomechanical process happen in the interferometer. We will show that Doppler friction will appear if we give up the approximation that the optomechanical coupling strength is a frequency independent constant. We also give the interpretation of Doppler friction in terms of the unbalanced Stokes and anti-Stokes sidebands. In section 3, we extend our discussion to more general interferometer configurations. We show that besides Doppler friction, there is a much more important energy dissipation mechanism through the optical damping effect, pointing towards possible future avenues of detector design that are discussed in the conclusion of the paper.

2. Optomechanical interaction betwen light beam and mirror

In laser interferometer gravitational wave detectors the basic physical process inside it is the interaction between the light beam and the center of mass (CoM) degrees of freedom of the mirrors. The CoM motion of the mirrors, driven by gravitational waves, modulates the light beam and creates anti-Stokes (upper) and Stokes (lower) sidebands with frequency $\omega_c \pm \Omega$. Here, ω_c is the frequency of the carrier beam and Ω is the frequency of gravitational waves.

This modulation process can also be treated in the quantum picture as generation of Stokes and anti-Stokes photons by scattering between the carrier photon and mechanical phonon, which can be described by the following Feynman diagrams shown in Fig.1

From these Feynman diagrams, it is clear that if the rate of the anti-Stokes process is higher than that of the Stokes process, more phonons will be absorbed through anti-Stokes process than emitted through Stokes process. In this case, there is a net flow of mechanical energy into the light field, and vice versa.

A widely-held view of this modulation process is that the Stokes and anti-Stokes

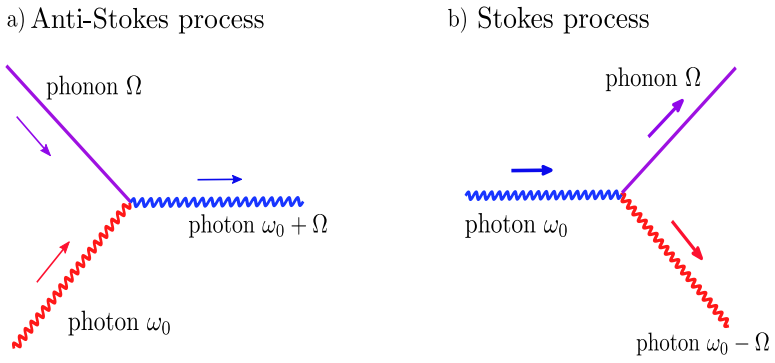

Figure 1. Parametric interaction in terms of Feynman diagram, (a) The anti-Stokes process, which causes a cooling effect by drawing a phonon out of the mechanical degrees of freedom (mirrors), creating an upper sideband photon with higher energy $\hbar(\omega_0 + \Omega)$; (b) The anti-Stokes process, creates a heating effect by emitting a phonon to the mechanical degrees of freedom, creating a lower sideband photon with lower energy $\hbar(\omega_0 - \Omega)$.

sidebands are 'balanced'. This means that the creation of an anti-Stokes sideband photon must be accompanied by the creation of a Stokes sideband photon. In other words, the photon generation rates of Stokes and anti-Stokes process are equal. Therefore according to this statement, there is no net energy transfer between mirror and optical field when a free propagating laser field is modulated by mirror motion.

In this section, by carefully analyzing a toy model, we want to show that this viewpoint is only approximately correct. What has been neglected here is the Doppler friction discussed by Braginsky and Saulson in [4] [5]. Firstly, we will derive the dynamics of the model, then we will try to develop an intuitive understanding of the result.

2.1. System Dynamics

First, we shall review the derivation of the optomechanical coupling Hamiltonian. For simplicity, we will start by discussing a toy model consists of a light beam reflected by a mirror, see Fig.2a. The light beam which is accompanied by quantum fluctuations is given by:

$$\begin{aligned} E_{in} = 2\sqrt{\frac{2\pi\hbar\omega_0}{Sc}}E_0\cos(\omega_0 t) + e^{-i\omega_0 t}\int_0^\infty \frac{d\Omega}{2\pi}\left(\sqrt{\frac{2\pi\hbar\omega_+}{Sc}}\hat{a}_+ e^{-i\Omega t} + \sqrt{\frac{2\pi\hbar\omega_-}{Sc}}\hat{a}_- e^{i\Omega t}\right) \\ + e^{i\omega_0 t}\int_0^\infty \frac{d\Omega}{2\pi}\left(\sqrt{\frac{2\pi\hbar\omega_+}{Sc}}\hat{a}_+^\dagger e^{i\Omega t} + \sqrt{\frac{2\pi\hbar\omega_-}{Sc}}\hat{a}_-^\dagger e^{-i\Omega t}\right). \end{aligned} \quad (1)$$

Here, ω_0 is the pumping frequency of the steady part of the incoming light beam, E_0 is the amplitude of steady field, S is its transverse cross-section. and $\hat{a}_\pm$ are the annihilation operators of the optical field at sideband frequency $\omega_0 \pm \Omega$. The first term here is the steady part of the optical field while the second part is the fluctuating part which has a continuous frequency distribution.

This optical field exerts a radiation pressure force $F = 2|E_{in}|^2 S/4\pi$ and does work on the mirror. Therefore the interaction Hamiltonian is: $H = -F \cdot x$. After substituting (1) and keeping the first order terms, we have:

$$H_{int} = -\frac{\hbar E_0}{c} \int_0^\infty \frac{d\omega}{2\pi} \sqrt{\omega_0 \omega} (\hat{a}_\omega e^{-i(\omega-\omega_0)t} + \hat{a}_\omega^\dagger e^{i(\omega-\omega_0)t}) \cdot x. \tag{2}$$

Here, we neglect the non-interesting steady part $\propto |E_0|^2 \hat{x}$ since it can be balanced by exerting an external constant force. We also rewrite $\hat{a}_{\omega_0 \pm \Omega}$ to be $\hat{a}_\omega$. This form of Hamiltonian can also be found in [12] [13].

It is important to notice that the coupling strength at frequency ω is now proportional to $\sqrt{\omega_0 \omega}$, a factor that comes from the beating between the steady and fluctuating optical amplitude. Usually, we treat $\omega \sim \omega_0$, thereby approximating the optomechanical coupling strength as a frequency independent constant. As we can see here, the coupling strength is not frequency independent. We will see that the approximation $\omega \sim \omega_0$ leads to the result that the two sidebands are balanced.

The Heisenberg equations describe the evolution of the mirror-field system are given by:

$$\frac{d\hat{a}_\omega}{dt} = i\frac{E_0}{c}\sqrt{\omega\omega_0}\hat{x}(t)e^{i(\omega-\omega_0)t}, \tag{3a}$$

$$\frac{dp}{dt} = \frac{\hbar E_0}{c} \int_0^\infty \frac{d\omega}{2\pi} \sqrt{\omega\omega_0} [\hat{a}_\omega^\dagger(t) e^{i(\omega-\omega_0)t} + \hat{a}_\omega(t) e^{-i(\omega-\omega_0)t}], \tag{3b}$$

$$\frac{dx}{dt} = \frac{p}{m}. \tag{3c}$$

First we consider the steady optical field and the fluctuating component due to modulation by the mirror motion, neglecting the quantum fluctuation field. We also assume an *initial condition* that at $t = 0$, there is no light except the pumping field at ω_0. Solving the above Heisenberg equations, we have:

$$\hat{a}_\omega(t) = i\frac{E_0}{c}\sqrt{\omega\omega_0} \int_{t_0}^t x(t') e^{-i(\omega-\omega_0)t'} dt', \tag{4a}$$

$$F_{rad} = m\frac{d^2x}{dt^2} = \frac{dp}{dt} = -\frac{2\hbar E_0^2 \omega_0}{c^2} \int_{t_0}^t dt' \int_0^\infty \frac{d\omega}{2\pi} [\omega x(t') \sin(\omega - \omega_0)(t' - t)]. \tag{4b}$$

Equation (4b) can be derived by substituting (4a) into (3b). Since $\omega = \omega_0 + \Omega$, and $v(t) = \Omega x(t)$ for harmonic motion with frequency Ω, therefore in (4b), we have a force term depend on Ω:

$$F_{rad}^\Omega = -\frac{2\hbar E_0^2 \omega_0}{c^2} \int_{t_0}^t dt' \int_{-\infty}^\infty \frac{d\Omega}{2\pi} \Omega x(t') \sin\Omega(t' - t). \tag{5}$$

Integrating by parts, and pick up the velocity dependent term which is related to the energy absorption, we have:

$$\hat{F}_v = -\frac{2\hbar E_0^2 \omega_0}{c^2} \dot{x}(t) = -\frac{2P\Omega}{c^2} v. \tag{6}$$

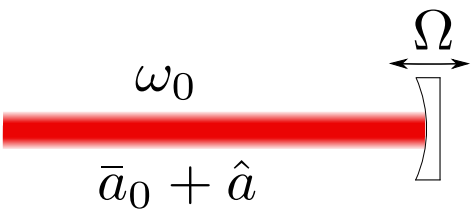

Figure 2. Our toy model of field-mirror interaction: the optical field is modulated by oscillating mirror with frequency Ω. Because of this modulation, the optical field consists of two parts, namely, the pumping part $\bar{a}$ and the sideband part $\hat{a}$

Following the logic of the above argument, we can easily see that if we impose the approximation $\omega \sim \omega_0$, we will not have the Ω-dependent radiation pressure term as in Eq.(5), and hence no above velocity dependent force.

The second equality of Eq.(6) comes from the fact that the power is given by $P = \hbar\omega_0|E_0|^2$ and the motion is a harmonic motion at Ω. Therefore Eq.(6) is exactly the Doppler friction force given in [5] and the appendix. For the real interferometer with arm cavities, we only need to multiply the above formula by the folding factor N_{fold} as in [5].

The above discussion shows that the Doppler friction factor given by Braginsky and Saulson emerges naturally when we use the Hamiltonian without the approximation of the frequency independence of the optomechanical coupling strength. Thus energy dissipation is a general phenomenon in interferometers. Its magnitude is only large in the case of detuned interferometer (see Section.3). A question then arises: since this Doppler friction effect is the result of opto-mechanical interaction, is there any way to use the quantum phonon-photon scattering picture (Fig.4) to explain it intuitively? In the next section, we will try to answer this question

2.2. Sideband photon generation rate

A more transparent way to investigate this toy model and answer the question raised in the end of the last section is to calculate the sideband photon generation rate explicitly. When the external force with frequency Ω drives the motion of the test mass (or the end mirror in our toy model discussed above), the optical fields in the sideband $\omega_0 \pm \Omega$ start to increase. The sideband photon generation rates are given by:

$$R_{\omega_0\pm\Omega}(t) = \langle i(t)|\hat{a}^\dagger_{\omega_0\pm\Omega}(t)\hat{a}_{\omega_0\pm\Omega}(t)|i(t)\rangle. \tag{7}$$

Here $|i(t)\rangle$ represents the sideband photon states. For the sidebands with their initial states as vacuum, we have:

$$|i(t)\rangle = \frac{1}{i\hbar}\int_0^t \hat{H}_{int}(t')dt'|0\rangle. \tag{8}$$

Here, the H_{int} is given in (2). Substituting into (7), after some simple algebra and integrating out all the $\delta-$funtions, we have:

$$R_\omega(t) = \frac{E_0^2}{c^2}\omega_0\omega x^2 = \frac{P}{\hbar c^2}\omega x^2. \tag{9}$$

From this, we can see that $\omega_0 \pm \Omega$ sideband-photon generation rates are not balanced if we do not approximate $\omega \sim \omega_0$. This gives us an the answer of the question raised in the last subsection. The Doppler friction effect can also be explained as the result of the unbalance between the rates of Stokes and anti-Stokes process. This unbalance is due to the frequency dependence of the optomechanical coupling constant ($\propto \sqrt{\omega\omega_0}$). To test our statement, the difference of $\omega_0 \pm \Omega$ sideband photon generation rates is:

$$R_{\omega_0+\Omega}(t) - R_{\omega_0-\Omega}(t) = 2\frac{P\Omega}{\hbar c^2}x^2. \tag{10}$$

This is also the phonon dissipation rate according to the particle number conservation. Multiplied by unit phonon energy $\hbar\Omega$, we have the mechanical power dissipated from test mass as:

$$\mathcal{P}^m_{diss} = \hbar\Omega[R_{\omega_0+\Omega}(t) - R_{\omega_0-\Omega}(t)] = 2\hbar\frac{P\Omega^2}{\hbar c^2}x^2 = 2\frac{P\Omega^2}{c^2}x^2. \tag{11}$$

Remembering that the frictional power dissipated is given by $F_v v$, and using $x = hL$ where h is the gravitational wave strain, and L is the length of the arm cavity, we can substitute in Eq.(6) to obtain:

$$P_v = -\frac{2P\Omega^2}{c^2}h^2L^2. \tag{12}$$

This result exactly matches with (11). This also can be seen as the result of energy conservation: the energy flow out of the test mass should flow into the optical field, that is: $P_v + \mathcal{P}^m_{diss} = 0$ as we can see by adding the right hand side of Eq.(11) and (12).

The above calculation of the sideband photon generation rate shows that conventional interferometers commonly thought to have balanced sidebands are not precisely balanced in reality. The unbalance arises because of the frequency-dependence of the optomechanical coupling constant, and is also the reason for the Doppler friction effect.

As we know, these sideband fields, which carry the gravitational wave information, will leak into the dark port of the interferometer and be measured by the photo-detectors. The total power of these sideband optical fields is given by:

$$P_{total} = P_+ + P_- = \frac{2P}{c^2}\omega_0^2\hat{x}^2 + \frac{2P}{c^2}\Omega^2x^2, \tag{13}$$

in which the first term represents the usual sideband energy that carries the displacement information of the end mirror by the gravitational waves. However, the second term is the power transferred from the test masses to the the optical field through Doppler friction (see Eq.(12)). This measures the velocity response of the test mass. Both of these two terms are needed to describe the output of the interferometer. From this analysis it is clear that the sideband power is not amplified Doppler friction power as previous analysis suggested [5].

3. Energy absorption in general configurations of interferometer

So far we have discussed Doppler friction in a simple but fundamental light-mirror interaction model. The energy absorption through Doppler friction is extremely small even if arm cavities like those used in LIGO type detectors are used to enhance the intracavity power. However, in more general interferometer configurations the energy absorption can be much larger. Many new interferometer configurations have been proposed, mainly to allow the free-mass standard quantum limit to be beaten through modifying the dynamics of test masses by opto-mechanical interaction. [2] [3] [7] [10]. In the following discussion we will show that these configurations actually increase the energy absorption from the gravitational wave signal through the creation of unbalanced sidebands. This is achieved by detuning the laser frequency with respect to the resonant point of interferometer. We note that detuning induced sideband unbalance is fundamentally different from the unbalance that occurs in Doppler friction, which is due to the frequency dependence of optomechanical coupling strength.

To formulate the problem, we start from the basic structure of a general interferometer configuration: a detuned cavity with a movable end mirror. For example, a signal recycling laser interferometer shown in Fig.3(a) can be mapped to a detuned cavity given in Fig.3(b). This mapping relation, as we shown in (Fig.3) is exactly proved in Buonanno and Chen [10] through treating the signal recycling cavity as an effective mirror. By tuning the signal recycling mirror, this signal recycling configuration can goes to the basic configuration considered in [5].

Here, we want to calculate the sideband photon generation rate and its associated mechanical damping factor which may be positive or negative. The effective cavity in Fig.3 has a spectral profile such as the one shown in Fig.4. Detuning of the laser frequency from the cavity resonance leads to unbalanced sidebands. A feedback loop diagram shown in Fig.5 can explain how the detuning creates positive or negative damping. A monochromatic gravitational wave at frequency Ω acts on the interferometer and causes the test mass to oscillate. The modulation causes the Stokes and anti-Stokes sidebands to build up inside the system. Both sidebands beat with the main beam and induce an AC radiation pressure force. However, the Stokes sideband radiation pressure is in phase with the velocity of mechanical motion, while the anti-Stokes radiation pressure has π phase shift relative to the velocity of mechanical motion. Thus the Stokes sideband represents positive feedback and can cause parametric instability (or heating, anti-damping), while the latter one causes cooling (or damping). When an interferometer is unbalanced, its Stokes sideband becomes higher than its anti-Stokes sideband. This causes the net feedback driving of mechanical modes to be non-zero. By changing the detuning, we change the relative strength of cooling and heating radiation pressure force.

To analyze the system quantitatively we start by writing the Hamiltonian of the system of Fig.3(b) in terms of the optomechanical coupling constant $G_0 = \omega_0/L$ and the cavity bandwidth γ. The bandwidth γ is given by $cT/4L$, where T is the transmissivity,

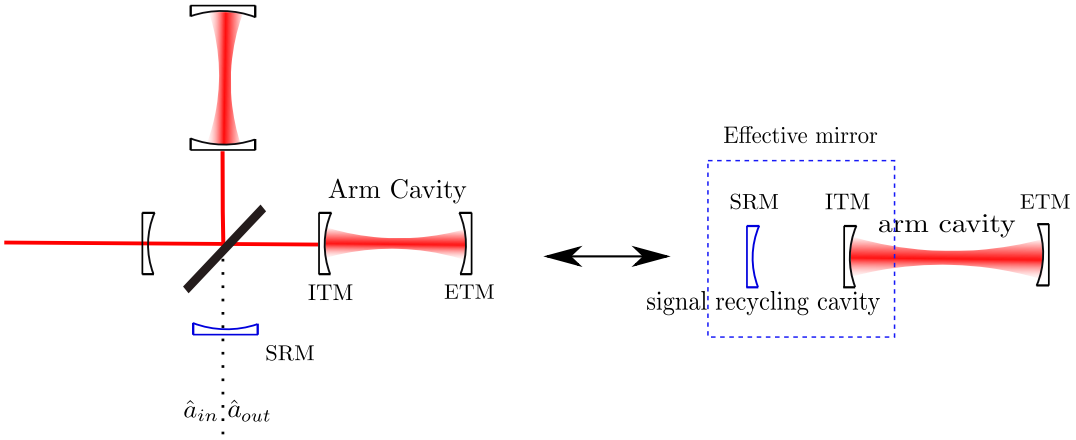

a) Signal Recycling Interferometer b) Detuned Fabri-Perot Cavity

Figure 3. A laser interferometer gravitational wave detector shown schematically in (a), treated using a simplified model consisting of a 3-mirror cavity. In (a) figure, ITM is the input test mass, ETM is the end test mass. PRM, SRM are the power recycling mirror and signal recycling mirror respectively. The common mode represented by the solid lines represent the pumping field to the cavity, while the dotted line represents the differential mode which carries the gravitational signal. Reference [10] shows that the signal recycling interferometer can be mapped to an effective detuned cavity shown in (b) if we treat the signal-recycling cavity as an effective mirror. The SRM here will introduce detuning of the effective cavity. For a continuous monochromatic gravitational wave signal , the carrier light, test mass and the two sidebands can be treated as four oscillators

L is the cavity length and c is the speed of light. In the Hamiltonian, $\hat{a}$ and $\hat{a}_{in}$ are the annihilation operators for the cavity field and the pumping field, while $\hat{p}$ and $\hat{x}$ are the momentum and displacement operators for the test mass. The frequency Ω, ω_c and ω_0 are the oscillation frequency of test mass motion which is the gravitational wave frequency, the cavity resonant frequency, and frequency of the pumping light respectively. Here, let us first put the tiny Doppler friction effect aside, and focus on the optical damping. In this case it is valid to impose the approximation that optomechanical coupling strength is a frequency-independent quantity.

The Hamiltonian can be written as [9]:

$$H = \hbar\omega_c \hat{a}^\dagger \hat{a} + p^2/2m + \hbar G_0 x \hat{a}^\dagger \hat{a} + i\hbar\sqrt{2\gamma}(\hat{a}_{in}\hat{a}^\dagger e^{-i\omega_0 t} - h.c.) - F_{GW} \cdot x. \tag{14}$$

Here, $-F_{GW} \cdot x$ is the work done by gravitational wave tidal force on the test mass and $F_{GW} = (1/2)\ddot{h}L$. From the above Hamiltonian, we obtain the linearized equations of motion:

$$m\ddot{x}(t) = -\hbar\bar{G}_0[\hat{a}^\dagger(t) + \hat{a}(t)] + F_{GW}(t), \tag{15a}$$

$$\dot{\hat{a}}(t) + (\gamma - i\Delta)\hat{a}(t) = -i\bar{G}_0 x(t) + \sqrt{2\gamma}\hat{a}_{in}(t). \tag{15b}$$

Here, $\bar{G}_0 = G_0\bar{a}$ while $\bar{a}$ is the steady amplitude of the cavity mode and Δ is the detuning

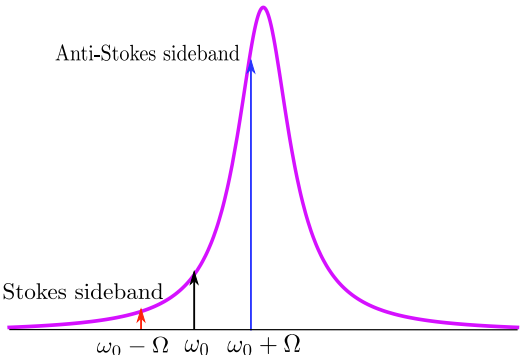

Figure 4. Unbalanced cavity spectral profile in the case of blue detuning. The black, red and blue arrows are the injection beam, Stokes sideband light and anti-Stokes sideband light respectively. The pink curve is the cavity spectral profile. The Stokes and anti-Stokes sidebands are created with different amplitudes due to the frequency dependence of the cavity response.

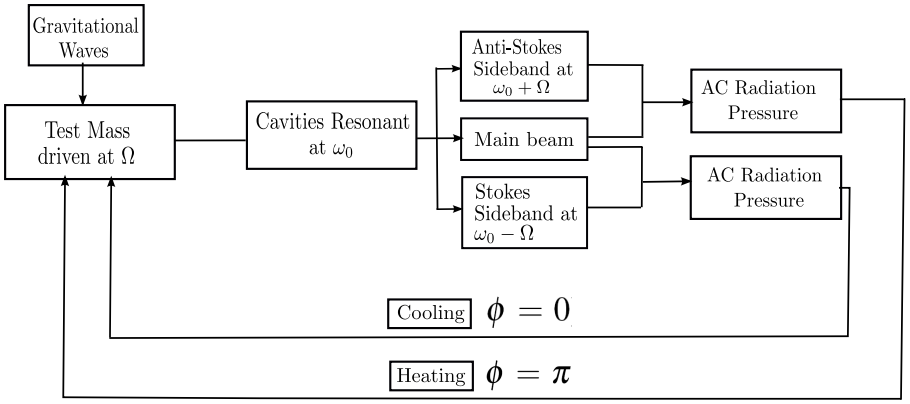

Figure 5. feedback flow chart of cooling and heating effect: a gravitational wave modulates the cavity field by driving the motion of the test mass, creates Stokes and anti-Stokes sidebands. The beating of these sidebands with the main laser beam will create radiation pressure force which back-act on the test mass. The radiation pressure force from the beating between anti-Stokes and Stokes sidebands are differed by a phase of π, which will contribute to the cooling and heating of mechanical motion

factor defined as $\Delta = \omega_0 - \omega_c$. This detuning can be experimentally realized by tuning the reflectivity and phase of the signal-recycling mirror.

Taking a Fourier transform of above equations, we obtain the following relations:

$$m\Omega^2 x(\Omega) = \hbar\bar{G}_0(\hat{a}(\Omega) + \hat{a}^\dagger(\Omega)) - F_{GW}(\Omega), \tag{16a}$$

$$\hat{a}(\omega) = \frac{\bar{G}_0 x(\omega)}{\omega + \Delta + i\gamma} + \frac{i\sqrt{2\gamma}a_{in}(\omega)}{\omega + \Delta + i\gamma}. \tag{16b}$$

The feedback processes shown in Fig.5 are described by Eq.17(a)(b). The first term on the right hand side of Eq.17(b) describes the affect of the external force driven mechanical motion on the optical field which in turn is feedback to the mechanical

motion through the radiation pressure force given by the first term on the right hand side of Eq.17(a).

Now we can derive the sideband photon generation rate using perturbation methods. We divide the Hamiltonian into two parts: a) the unperturbed part consisting of the optical cavity and the mechanical oscillator, and b) the interaction term $\hbar G_0 x \hat{a}^\dagger \hat{a}$ representing the perturbed part. Using the Fermi Golden Rule, which states that the transition rate is proportional to the square of expectation value of perturbed Hamiltonian, this calculation was given by Marquardt et.al [11]. We give a review of their procedure here: defining the (anti-)Stokes process rate as $R^{\text{(anti-)Stokes}}$. Since the mechanical (anti-)damping rate $\Gamma^{\text{(anti)-Stokes}}$ measures the relative mechanical energy (gain) loss per unit time ($dE_m/E_m dt$) where $dE_m/dt = \hbar\Omega R^{\text{(anti-)Stokes}}$, it follows that:

$$\Gamma^{\text{Stokes}} = -\frac{\hbar\Omega R^{\text{Stokes}}}{E_m}.$$

The energy change per unit time is just the unit phonon energy times the rate of the Stokes process. The same applies for anti-Stokes process. Then we have:

$$\Gamma^{\text{Stokes}} = \frac{\hbar\Omega R^{\text{Stokes}}}{E_m} = \frac{\hbar\Omega}{\hbar\Omega\bar{n}_m}\frac{(\hbar\bar{G}_0)^2}{\hbar^2}|\langle f|x|i\rangle|^2\langle\hat{a}\hat{a}^\dagger\rangle_{\omega=\Omega} = \bar{G}_0^2\frac{\hbar}{2m\Omega}\frac{2\gamma}{(\Omega-\Delta)^2+\gamma^2}. \quad (17)$$

In deriving this formula, we should substitute (17b) into $\langle aa^\dagger\rangle$ and the free evolution solution of (17a) into $|\langle f|x|i\rangle|^2$.

For the anti-Stokes process:

$$\Gamma^{\text{anti-Stokes}} = \frac{\hbar\Omega R^{\text{anti-Stokes}}}{E_m} = \frac{\hbar\Omega}{\hbar\Omega\bar{n}_m}\frac{(\hbar\bar{G}_0)^2}{\hbar^2}|\langle f|x|i\rangle|^2\langle\hat{a}\hat{a}^\dagger\rangle_{\omega=-\Omega} = \bar{G}_0^2\frac{\hbar}{2m\Omega}\frac{2\gamma}{(\Omega+\Delta)^2+\gamma^2}. \quad (18)$$

According to the particle conservation law, we have:

$$\Gamma^{\text{phonon}} = \Gamma^{\text{anti-Stokes}} - \Gamma^{\text{Stokes}}. \quad (19)$$

This tells us that the mechanical damping rate Γ^{phonon} is given by the difference between Eq.(18) and Eq.(19), which can be simplified to:

$$\Gamma^{\text{phonon}} = -\bar{G}_0^2\frac{\hbar}{m}\frac{2\Delta\gamma}{[(\Omega-\Delta)^2+\gamma^2][(\Omega+\Delta)^2+\gamma^2]}. \quad (20)$$

This result is equivalent to the optical damping factor given as the imaginary part of optical rigidity in [10, 9]. For a typical interferometer cavity used in gravitational wave detection, we plot the form of Γ^{phonon} as a function of cavity detuning Δ in Fig.6. When $\Delta > 0$, the optical damping factor is positive and the radiation pressure force fed back to mechanical motion has the form of $F = m|\Gamma^{\text{photon}}|\Omega x(\Omega)$. It is in-phase with the velocity of mechanical motion, and induces the heating effect shown in Fig.(5). However when the $\Delta < 0$, the radiation pressure force has the form of $F = -m|\Gamma^{\text{photon}}|\Omega x(\Omega)$. It differs by a π phase shift, thereby driving the mechanical motion in anti-phase which

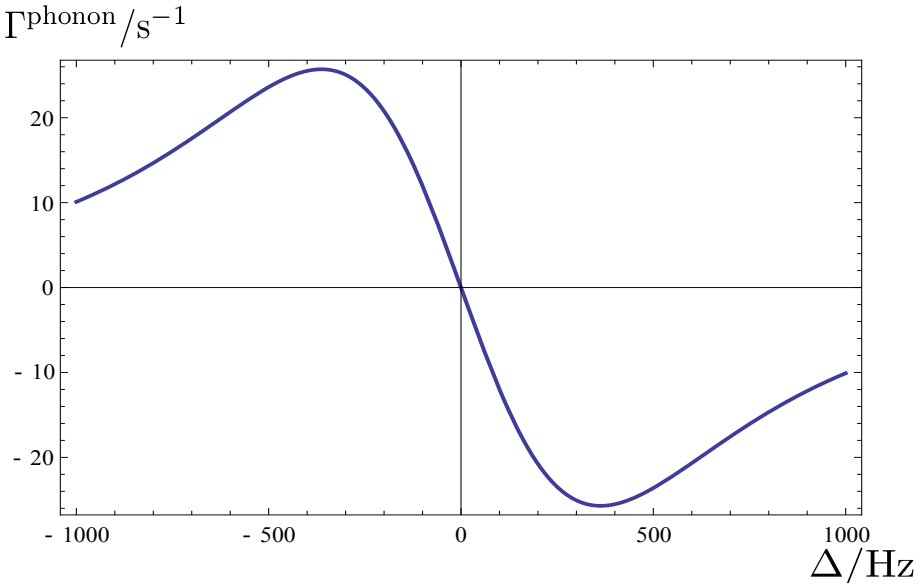

Figure 6. The relationship between the optical damping rate Γ^{phonon} and the detuning Δ. When $\Delta < 0$, the optical damping is positive and corresponds to optomechanical cooling while $\Delta > 0$, the optical damping is negative and corresponds to optomechanical heating. Here, we take the typical interferometer cavity parameters: cavity bandwidth is 100Hz, mirror mass is 40kg, intracavity photon number is 10^{20} and cavity length $\sim$ 4000m

induces cooling. When there is no detuning (i.e. $\Delta = 0$), then the transition rates become equal such that the total optomechanical damping rate is zero:

$$\Gamma^{\text{Stokes}} = \Gamma^{\text{anti-Stokes}} = \bar{G}_0^2 \frac{\hbar}{2m\Omega} \frac{2\gamma}{\Omega^2 + \gamma^2}. \tag{21}$$

In this case the anti-Stokes sideband and Stokes-sideband rates are exactly cancelled with each other and $\Gamma^{\text{phonon}} = 0$ (under the frequency-independent coupling strength approximation). This corresponds to the case illustrated in Fig.5, in which the cooling and heating terms cancel each other. Under these circumstances the test masses can be treated as free masses except for the negligible Doppler friction. These results are not only correct for the near-resonance case such as the one shown in Fig.4, but also correct for more general cavity field structure such as the case discussed further below in which a single sideband is resolved and resonant with a high order mode. An analogous single sideband device that manifests the above behaviour has recently been experimentally demonstrated by Chen.et.al [17].

Note that the optical damping factor Γ^{phonon} is always associated with the optical spring effect, and for the system with optical-damping, the associated optical spring constant is always negative and hence can lead to instability. These relations were discussed by Buonanno et.al [10]. However, this instability problem can be solved using the double-optical spring configuration proposed by Rehbein et.al [15] or by an electronic feedback loop as proposed by Buonanno et.al [10]. Once stabilised, an optical

spring interferometer operates like a resonant mass gravitational wave detector. The mechanical stiffness of this detector is contributed by the optical field.

For the optical spring interferometer, we can calculate the energy in the gravitational wave detector following results already derived long ago by Misner Thorne and Wheeler [18] for resonant bar detectors. The steady state vibration energy of the test masses is given by:

$$E_{kin} = \frac{mL^2h^2\Omega^6}{16[(\Omega^2 - \omega_{\rm opt}^2)^2 + \Omega^2\Gamma_{\rm eff}^2]}. \tag{22}$$

Here, the interferometer is treated as a mechanical quadrupole oscillator with a resonant frequency $\omega_{\rm opt}$ due to optical rigidity and L, h and Ω are the length of the arm cavity, strain and frequency of the gravitational wave. The effective test mass damping rate $\Gamma_{\rm eff}$ is equal to the effective bandwidth of the oscillator. For the double optical spring interferometer the damping is contributed by the superposition of two optical springs ($\Gamma_{\rm eff} = \Gamma_1^{\rm phonon} + \Gamma_2^{\rm phonon}$) [3]. For a feedback stabilised optical spring interferometer the damping is contributed by the sum of optical anti-damping factor and damping rate contribute by the electronic feedback loop ($\Gamma_{\rm eff} = \Gamma^{\rm phonon} + \Gamma_{\rm feedback}$) [10].

The steady state kinetic energy (assuming a continuous gravitational wave source) is dissipated internally at a rate $E_{kin} \cdot \Gamma^{\rm eff}$, which is the energy absorption rate of the detector, or the average absorbed power from the gravitational waves by the detector [18]. The average absorbed power, derived from Eq.22 is shown in Fig.7 for a sinusoidal gravitational wave of amplitude 10^{-23} in a typical advanced interferometer. From this, we can see that when the gravitational wave frequency is resonant with the mechanical resonant frequency of the mass-spring system, the absorbed power is much higher. It can be 10^{15} times higher than to the Doppler friction power. Since the energy absorption cross section $\sigma = E_{kin} \cdot \Gamma^{\rm eff}/\mathcal{F}$ with $\mathcal{F}$ is the gravitational wave energy flux, the σ is also relatively high ($\sim 10^{-22}{\rm m}^2$) when the mechanical resonant frequency of the interferometer is resonant with the gravitational wave frequency.

Moreover, we need to point out that the Doppler friction power also gets amplified when the detector is resonantly driven by gravitational waves as what has been discussed in the last section. The reason is that the Doppler friction power, as shown in Eq.(11), depends on the oscillation amplitude. Estimation shows that the Doppler friction power is still $\sim 10^{12} - 10^{15}$ smaller, thereby it is negligible.

Since detuning induced sideband imbalance leads to strong energy absorption from gravitational waves, it is interesting to consider other detector designs that can be dominated by a single sideband. One interesting idea is the tilt interferometer [6]. Unlike the ordinary design of interferometer configuration which measures the + mode of gravitational waves, this idea aims to detect the $\times$ mode of gravitational waves. In this case, the test mass rotation due to the $\times$ mode of gravitational waves will scatter the laser field into a $\rm TEM_{01}$ spatial mode with frequency $\omega_0 - \Omega$. The signal recycling mirror is designed to make the resonant frequency of the differential mode match the high-order-mode, thereby increasing the gravitational wave signal energy through strong

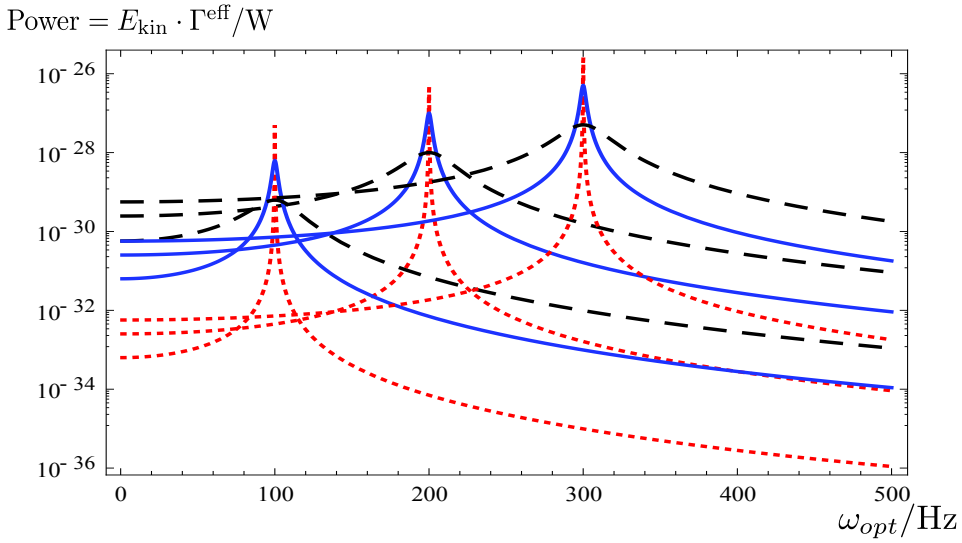

Figure 7. The average absorbed power in a double-spring interferometer as a function of optical spring frequency due to monochromatic gravitational waves of frequency 100Hz, 200Hz and 300Hz and $h \sim 10^{-23}$. We assume a LIGO type interferometer. The graphs show the absorbed power as a function of optical spring frequency. for three different optical damping values.The red-dotted, blue-solid and black-dashed lines represent total optical damping $\Gamma_{\rm eff}$ of 0.4, 40 and 400 s^{-1} respectively.

angular optical damping. The upper sideband is suppressed due to the asymmetric mode structure of long optical cavities.

4. Conclusion

We have tried to clarify the conceptual understanding of the physics of gravitational wave detectors. Stimulated by previous work [4] [5], we have been able to obtain a unified understanding of gravitational wave energy absorption by laser interferometers, which combines the intrinsic, but tiny, Doppler friction term with an optical damping term which can be tuned by varying the relative amplitude of the signal sidebands.

We have shown that within the approximation that the optomechanical coupling strength is frequency-independent, conventional laser interferometer gravitational wave detectors with balanced sidebands such as LIGO can be treated as lossless parametric transducer in which the energy absorption from gravitational waves is zero. Beyond the assumption of frequency-independent optomechanical coupling strength, there exists an unavoidable but tiny Doppler friction term. The Doppler friction itself is explained by the Stokes and anti-Stokes sideband photon generation rates having a small unbalance caused by the frequency-dependent optomechanical coupling strength. For more general interferometer configurations such as the double optical spring interferometer, variation of the relative strength of the Stokes and anti-Stokes sidebands leads to strong optical damping and greatly enhanced absorption of gravitational wave energy. Our results were derived for monochromatic gravitational waves, but are true in general because

every wave can be treated as a superposition of monochromatic waves. The ability to tune the optical spring stiffness through the relative sideband amplitudes is analogous to the variation in in-phase and anti-phase signal feedback used in electronic amplifiers, where variation of the feedback is used to change the gain and the input impedance of the amplifier. The design of gravitational wave detectors can be considered from the same viewpoint. By changing the optical spring stiffness of the test masses, we change the mechanical input impedance of the interferometer. Because of the extremely high impedance of free space $\sim c^3/G$, laser interferometers are always poorly impedance matched to gravitational waves. However by increasing the optical stiffness we increase the input impedance, thereby reducing the impedance mismatch with free space and increasing the fraction of absorbed energy. The results presented here imply that a single sideband gravitational wave detector would be advantageous, and we propose to explore possible designs that could achieve this. We note that practical designs must take into account numerous technical noise issues which can overwhelm the in-principle advantages we have discussed here.

5. Acknowledgement

We thank fruitful discussion with Haixing Miao, Peter Saulson, Harald Luck, Farid Ya Khalili, Yanbei Chen, Huan Yang, Maxim Goryachev, Sergey P Vyachatnin, and Stefan.L.Danilishin. Y.Ma is supported by the Australian Research Council and the Department of Education, Science and Training.

References

[1] *General Relativity and Gravitational Waves* by Joseph Weber, New York Interscience. 1961
[2] *Traveling at the speed of Thought* by Daniel Kennefick,Princeton.2007
[3] Hermann Bondi, Nature 179 (4569):1072-1073, 1957.
[4] Braginsky V.B. and Manukin A.B. Soviet Physics JETP 25,653 1967.
[5] Peter R Saulson, Class.Quantum.Grav.14:2435-2454,1997.
[6] Blair. D.G. et.al Single sideband angular deflection gravitational wave detector (in preparation)
[7] Braginsky V.B, Gorodetsky M.L and Khalili F.Ya,Phys Lett A 232,5,340-348,1997
[8] Manley J.M and Rowe H.E Proc.TRE 44 904,1956
[9] Haixing Miao, Stefan Danilishin, Helge Muller-Ebhardt and Yanbei Chen New J. Phys. 12 083032,2010
[10] A. Buonanno and Y. Chen, Phys. Rev. D65 042001.
[11] Marquart F, Chen J.P,Clerk A.A and Girvin S.M, Phys Rev Lett 99, 093902.2007
[12] Braginsky V.B, Gorodetsky M.L, Khalili F.Ya, Matsko A.B, Thorne K, and Vyatchanin S.P, Phys Rev. D 67, 082001, 2003
[13] S.L.Danilishin and F.Ya.Khalili, Living Rev. Relativity 15, 5. 2012
[14] *Quantum Optics* by Scully M.O and Zubairy M.S Cambridge University Press,1999
[15] Rehbein H, Mller-Ebhardt H,Somiya K.Danilishin S.L, Schnabel R,Danzmann R, and Chen Y.Phys. Rev. D 78, 062003 2008
[16] Hild S and Freise A, Class.Quantum.Grav. 24 5453-5460 2007
[17] Xu.Chen et.al. private communication.

[18] C. W. Misner, K. S. Thorne and J. A. Wheeler *Gravitation*, San Francisco: W.H. Freeman and Co., 1973

Appendix A. Derivation of Doppler friction by Lorentz transformation

In this appendix, we are going to give an exact derivation of Doppler friction by Lorentz transformation of the electromagnetic wave field. This derivation is provided by William Kells, and gives exactly the same result as Eq.(12).

Considering the same toy model shown in Fig.2. For perfectly conducting surface with boundary position $X = x\cos\Omega t$, the expression for the reflective electric field E_{Rfl} can be written as:

$$E_{ref}(X = x\cos\Omega t, t) = -E_0 e^{ik_0 X + i\omega_0 t} e^{-2ik_0 x\cos\Omega t}. \tag{A.1}$$

It could be more rigorous to take boundary conditions of Maxwell equations in the boundary's rest frame. In the case of inertial mirror motion $x = vt$, imposing this rest frame boundary conditions, we have:

$$E_{ref} = -\frac{1-\beta}{1+\beta} E_0 e^{i(k_0 x + \omega_0 t)\frac{1-\beta}{1+\beta}}, \tag{A.2}$$

with $\beta = v/c$. This is exactly what would be expected physically: The reflected wave is Doppler shifted in frequency by $\sim (1-2\beta)$, and the reflected waves's Poynting vector is reduced by $\sim (1-4\beta)$. In this case, the reflected light has lost power, which means the light field does work on the mirror at rate $2c|E_0|^2\beta$. Second, the receding mirror in the laboratory frame leaves a growing path of "stored" beam energy in its wake, effectively absorbing power $2|E_0|^2\beta c$. The factor $(1-\beta)/(1+\beta)$ in the above equation accounts for these losses.

In case of periodic motion at frequency Ω which is of interest to gravitational wave detector, these power flows at the order of β will just be averaged to zero. Thereby expansion to β^2 need to be kept. For slow periodic motion, during the first half-cycle motion, the reflected beam energy passing a fixed reference plane is:

$$U_1 = P_0 \left(\frac{1-\beta}{1+\beta}\right)\left(\frac{x}{c\beta} + \frac{x}{c}\right), \tag{A.3}$$

during the second half cycle motion when the velocity of the mirror changes direction, it is given by:

$$U_2 = P_0 \left(\frac{1+\beta}{1-\beta}\right)\left(\frac{x}{c\beta} - \frac{x}{c}\right). \tag{A.4}$$

Then the correct power flow per cycle (the period is equal to $2x/c\beta$) is then:

$$P_{cycle} = \frac{U_1 + U_2}{2x/(c\beta)}. \tag{A.5}$$

Substitute Eq.(25) and (26) into Eq.(27), keep to the β^2 order and take the average over one cycle, we have:

$$P_{cycle} = P_0(1 + 4\langle\beta^2\rangle_{cycle}) = P_0(1 + 2\frac{\Omega^2}{c^2}x^2). \tag{A.6}$$

This result is exactly match to Eq.(12) in the main text.